A particle-on-a-sphere model for C_{60}

Michael R. Savina, Lawrence L. Lohr and Anthony H. Francis

Department of Chemistry, University of Michigan, Ann Arbor, MI, 48109, USA

A perimeter model for the π electrons of C_{60} is developed and implemented within the independent particle approximation. Physically, the model gives the energy levels of a particle on a sphere perturbed by the icosahedral potential set up by the 60 carbon atomic cores. Computational techniques are adapted from well known crystal field formalisms. The molecular orbitals are represented by linear combinations of spherical harmonics. One or two adjustable parameters are used to give reasonable agreement with the observed UV–visible spectrum and with semi-empirical and ab initio calculations at a similar level of approximation. A closed-shell ground state, appreciable HOMO–LUMO gap, and electric dipole forbidden HOMO–LUMO transition are predicted.

1. Introduction

Since its discovery in 1985 [1], C_{60} has been the subject of many quantum-mechanical calculations [2–9]. Techniques ranging from Hückel theory to rigorous Hartree–Fock SCF computations have predicted the two distinct bond lengths, closed-shell ground state and appreciable HOMO–LUMO gap observed experimentally. In addition, papers which report results at the orbital level are in agreement as to the ordering of the molecular orbitals in terms of energy. These calculations have provided much useful information about C_{60} but fail to give a simple conceptual basis for understanding the electronic structure of the molecule. Many of the authors have addressed this issue by noting the similarity between the energy levels of the C_{60} π system and those of a particle on a sphere [2–4,7–9]. We present here an elaboration of this idea, in which the π electrons are treated as independent particles sliding on the surface of a sphere onto which is impressed an icosahedral potential generated by point charges at the carbon atomic positions. The present treatment is restricted to this conceptually simple case and ignores electron correlation. The predictions are therefore limited to results at the orbital level of approximation.

The concept of idealizing structures in this way was developed for two-dimensional systems some time ago. A perimeter model for cata-condensed hydrocarbons (benzene, naphthalene, anthracene, etc.) was first proposed by Platt in 1949 [10]. The π electrons are treated as particles on a circle whose circumference is equal to the perimeter of the hydrocarbon in question. The resulting Schrödinger equation is that of a plane rotor. The actual shapes of the molecules were treated as perturbations both qualitatively [10] and quantitatively [11,12].

In the case of a particle on a sphere, the unperturbed problem is that of a rigid rotor. The well known solutions of the purely angular Schrödinger equation are the spherical harmonics, Y_l^m. The energy levels are given by the familiar expression

$$E(l) = \frac{l(l+1)\hbar^2}{2m_e r_0^2},\tag{1}$$

where m_e is the mass of the electron and r_0 is the radius of the sphere. When the levels are filled with the 60 π electrons of C_{60}, the HOMO and LUMO correspond to levels $l=5$ and 6, respectively. Given a radius of 3.51 Å [13], the first allowed transition predicted by this model is at 3.71 eV, in remarkable agreement with experiments that suggest 3.0–3.8 eV [14,15].

The unperturbed model gives many unrealistic predictions however, such as an open-shell ground

state and 11-fold degenerate HOMO. These problems are addressed by replacing the spherical potential with an icosahedral potential, which is generated by the carbon atomic cores. This potential breaks the degeneracies of all levels with $l \geqslant 3$. Simple group theory gives all the splitting patterns and shows that under the point group I_h the $l = 5$ level splits into three sets of orbitals, h_u, t_{1u}, and t_{2u}, with degeneracies of 5, 3, and 3, respectively. The closed-shell ground state can be accounted for by assuming the h_u orbitals lie lowest of these, however one does not know a priori the ordering of the orbitals or magnitude of the splittings. These properties can be readily calculated using a crystal field formalism.

2. Crystal field treatment

The purely Coulombic icosahedral potential is written as an expansion in spherical harmonics about the center of the sphere in a manner commonly employed in crystal field calculations via the following well-known expansion theorem [16]:

$$V = Ze \sum_i \frac{1}{|\mathbf{r} - \mathbf{r}_i|} \sum_{l=0}^{\infty} \sum_{-l}^{l} R_l(r) C_l^m Y_l^m(\theta, \phi) , \qquad (2)$$

where Ze is the effective charge on the carbon atomic cores and $\mathbf{r}$ and $\mathbf{r}_i$ are the vector coordinates of the electron and carbon atomic cores. The radial component is ordinarily given by

$$R_l(r) = \frac{r^l}{r_c^{l+1}} , \qquad (3)$$

where r and r_c are the radial coordinates of the electron and carbon atomic cores, respectively. Since the cores and electron are restricted to the surface of the sphere, $r = r_c = r_0$, and the right-hand side of eq. (3) reduces to simply $1/r_0$ for all l.

The coefficients of the angular terms in the potential expansion can be derived from group theoretical considerations. For instance, since C_{60} has inversion symmetry, no odd l terms may appear in the expansion. Choosing a fivefold axis as the axis of quantization and requiring that V transforms as the totally symmetric representation in the icosahedral point group, all terms vanish except those for which m is an integer multiple of 5 and l is an integer multiple of 6, 10 or 16. In principle, the angular coef-

ficients can be determined solely from the group theoretical arguments, but the high symmetry of C_{60} makes this technique extremely tedious. An alternate approach is to write the coefficients as expansions of spherical harmonics via the so-called "multipole expansion theorem" [16]

$$C_l^m = \frac{4\pi Ze}{2l+1} \sum_i Y_l^{m*}(\theta_i, \phi_i) , \qquad (4)$$

where Ze is the effective charge on each carbon atomic core and θ_i and ϕ_i are the angular coordinates of the carbon atomic cores.

Eq. (2) is rigorously correct only when the summation over l extends from zero to infinity, however, the summation can be truncated without affecting the matrix of the Hamiltonian in the region of interest. First, the $l = 0$ term can be neglected since it represents the purely spherical component of the potential and gives rise to no splittings. Second, terms in the potential for which the relationship

$$|l' - l''| \leqslant l \leqslant l' + l'' \qquad (5)$$

does not hold integrate to zero ("vector triangle rule") and can be omitted.

The matrix elements can be written as

$$\langle \Psi' | -eV | \Psi'' \rangle = -\frac{4\pi Ze^2}{r_0}$$

$$\times \sum_{l,m} \frac{\sum_i Y_l^{m*}(\theta_i, \phi_i)}{2l+1} \langle Y_{l'}^{m'} | Y_l^m | Y_{l''}^{m''} \rangle . \qquad (6)$$

Each term in the potential is even, so for the integrand to be an even function, $Y_{l'}^{m'}$ and $Y_{l''}^{m''}$ must be either both even or both odd. Therefore l' and l'' must differ by an even integer. Also, the integral vanishes unless $m + m'' - m' = 0$. Since group theory restricts m to integer multiples of 5, all matrix elements vanish except those for which $m'' - m'$ is also an integer multiple of 5.

A significant departure from a typical crystal field calculation is the size of the matrix of the Hamiltonian. Most crystal field calculations concern splittings of d or f orbitals and so include only the $l = 2$ or $l = 3$ levels. Given the $60\,\pi$ electrons of C_{60}, levels to $l = 5$ are occupied and even $l = 8$ is spectroscopically accessible. Furthermore, the angular momentum states are coupled strongly by the potential so that interactions between states cannot be ignored.

Whereas a typical crystal field Hamiltonian matrix contains 25 or perhaps 49 elements (for d or f orbitals, respectively), this matrix requires 50625 elements. Thus the group theoretical constraints are invaluable because they show that only a small fraction of the elements are non-zero and require evaluation. Taken together, the group theoretical constraints on l and m cause 90% of the matrix elements to vanish, greatly reducing the computational burden.

The parameter Ze, the effective charge on the carbon core, is not known a priori and must be fitted based on experimental results. In addition, a two-parameter fit can be obtained by replacing the electron mass in the kinetic part (eq. (1)) with an effective electron mass, as is commonly done in solid-state calculations to account for complications imposed by a periodic potential function.

The calculations were performed on a SGI 4D/360 computer. Matrix elements can be evaluated by a variety of methods including Wigner 3-j symbols [17], exact integration via a symbolic computation language, Maple V [*1], or numerical integration using Gaussian quadrature. The carbon nuclei positions were determined using $r_0 = 3.512$ Å, short bond length $= 1.388$ Å, and long bond length $= 1.433$ Å [13]. The largest matrix included levels up to $l = 14$, requiring terms to $l = 28$ in the potential expansion.

3. Results and discussion

Plots of orbital energies versus the effective charge (Ze) are shown in fig. 1. The electron mass is taken as the actual electron rest mass and the lowest-energy level is taken as the zero of energy with all other levels plotted relative to it.

The HOMO is shown as the heavy line in the $l = 5$ manifold of fig. 1a. The left side of the figure represents the physically unreasonable case of a negative effective core potential, and the ground state prediction is an open-shell t_{1u}^4 configuration. When Z is positive, the diagram predicts a closed-shell ground state configuration, h_u^{10}, in agreement with other calculations [2–9]. The HOMO–LUMO transition is a forbidden intraterm transition within the $l = 5$ manifold for values of Z less than one. In fact,

*1 Waterloo Maple Software, University of Waterloo.

in almost all cases one can quickly establish whether a given transition is allowed or forbidden simply by inspecting the parentage of the orbitals involved. The only exception is $2t_{1u} \leftarrow 1g_g$, which is forbidden on the basis of other symmetry considerations (this excitation does not give rise to a T_{1u} state, which is the only allowed one-photon excitation from the ground state). Calculated oscillator strengths agree with these observations. In addition, fig. 1b shows the orbitals separating into two bands as the effective charge grows. The lower levels are stabilized by the perturbing potential, while the upper levels are destabilized by it.

A consequence of the strong coupling between states described in section 2 is the region near the HOMO was observed to change as the number of angular momentum states in the matrix increased. Given the high symmetry, it is necessary to include states of very high angular momentum to be sure that a representative sample of each symmetry species has been obtained. A conspicuous example is the t_{2g} orbital set of the $l = 8$ manifold ($1t_{2g}$). It is the first of its species to appear and so interacts with nothing below itself. When one other t_{2g} orbital is introduced by extending the calculation to include $l = 10$ ($2t_{2g}$), the interaction is so strong that $1t_{2g}$ drops rapidly, crossing the HOMO at an effective charge of 1.1 (fig. 1b). The diagram continues to change as higher levels are introduced, but becomes invariant when 14 levels are included in the matrix.

The behavior of $1t_{2g}$ seems somewhat disconcerting at first; there are nine orbitals which are the first of their respective species to appear, yet $1t_{2g}$ drops quite precipitously compared to the other eight. Braga et al. [8,9] calculate the energy of this orbital at about 2.7 eV above the LUMO, which corresponds to about $Z = 0.8$ in fig. 1b. They label it $2t_{2g}$, from which we infer there is an orbital with t_{2g} symmetry in the σ set, which presumably prevents it from dropping even further.

To better understand the behavior of $1t_{2g}$ it is necessary to inspect the molecular orbitals themselves. We show in fig. 2 a plot of electron density for the sum of the three degenerate eigenstates that make up $1t_{2g}$. Under a weak perturbation (low effective charge), the electrons are distributed primarily in the pentagons and the centers of the hexagons. As the charge is increased they move rapidly to the carbon
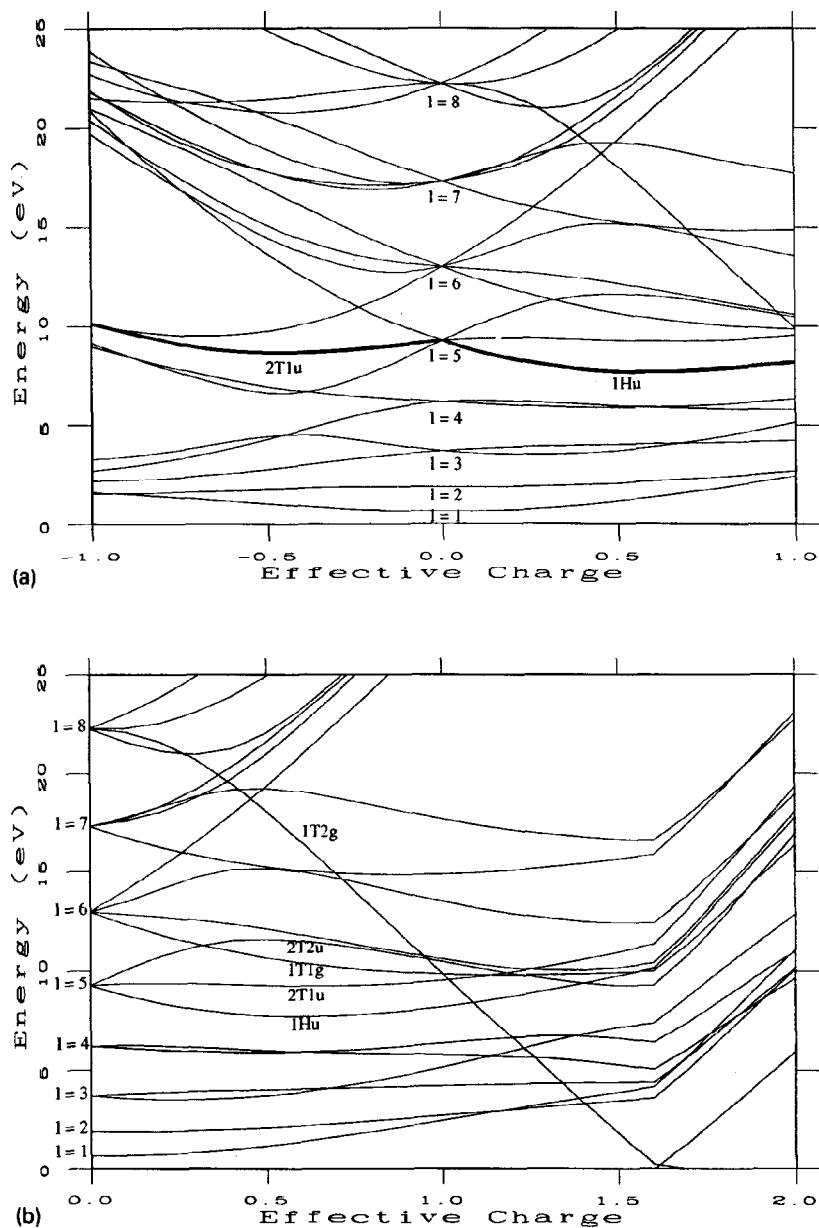
Fig. 1. Orbital energies as a function of the effective charge on each carbon atom experienced by an electron moving on the surface of C_{60}. The heavy line in part (a) is the HOMO. The zero of energy is taken as the lowest energy level at any given effective charge.

atomic core positions. The highly noded character of the orbitals indicates it originates in a high angular momentum state, but the situation of the anti-nodes precisely at the atomic core positions results in a po-

tential stabilization which dominates the kinetic term and lowers the energy dramatically.

Spectral assignments by Leach et al. [14] were used for fitting the parameters Z and m_{eff}. Table 1 gives
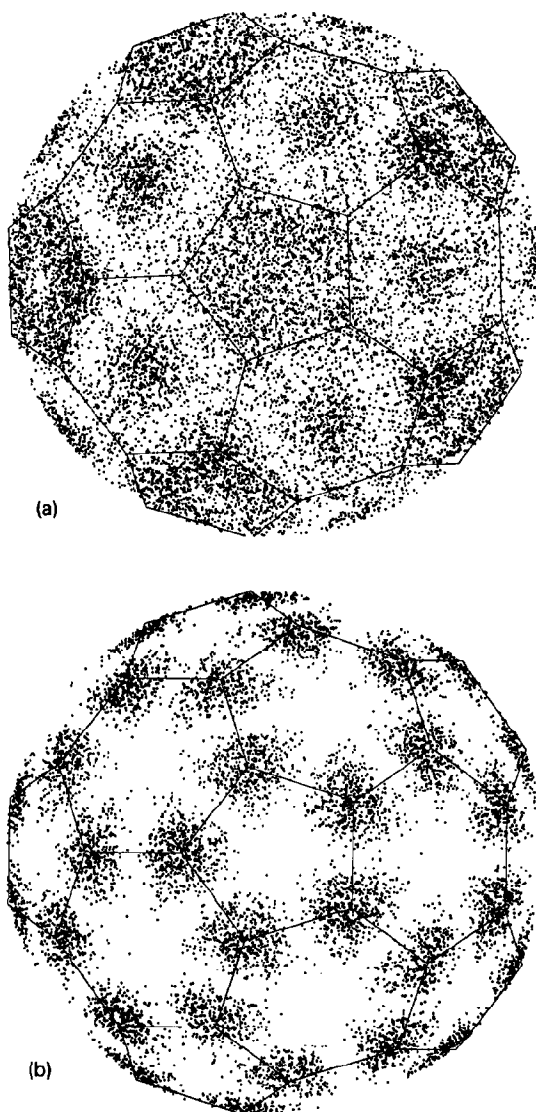
(a)

(b)

Fig. 2. Electron density plots for the sum of the three orbitals of $1t_{2g}$ at effective charges of (a) 0.0001 and (b) 0.88. The view is along a fivefold axis and shows only half of the molecule. Dot density corresponds to electron density.

the fits considering *only* allowed transitions. Note the unusual feature that most of the transitions originate below the HOMO.

The best fit for the single parameter model was found at $Z=0.88$, with a total deviation from the observed peak positions of 4.02 eV. This puts most of

Table 1
Allowed transitions in C_{60}: observed and calculated energies

Obs. (eV) [a]	One-parameter fit		Two-parameter fit	
	this work	assignment	this work	assignment
3.14	1.98	$1h_u \rightarrow 1t_{1g}$	2.20	$1h_u \rightarrow 1t_{1g}$
3.29	3.01	$1h_u \rightarrow 3h_g$	2.44	$2h_g \rightarrow 2t_{1u}$
3.78	3.21	$2h_g \rightarrow 2t_{1u}$	3.22	$1h_u \rightarrow 3h_g$
4.07	3.91	$1h_u \rightarrow 1t_{2g}$	3.96	$1g_g \rightarrow 2t_{2u}$
4.36	4.68	$2h_g \rightarrow 2t_{2u}$	4.06	$2h_g \rightarrow 2t_{2u}$
4.84	5.03	$1g_g \rightarrow 2t_{2u}$	5.22	$1h_u \rightarrow 2g_g$
5.46	5.99	$1h_u \rightarrow 2g_g$	5.22	$1h_g \rightarrow 2t_{1u}$
5.89	6.27	$1t_{2u} \rightarrow 3h_g$	5.97	$1g_u \rightarrow 3h_g$
6.37	6.80	$1g_u \rightarrow 3h_g$	6.24	$1t_{2u} \rightarrow 3h_g$

[a] Ref. [14].

the transitions in the region between 3 and 6 eV, in good qualitative agreement with the spectrum. Fig. 3 is a Mulliken diagram of the orbital energies. The orbital ordering is in agreement with other calculations from HOMO−2 to LUMO+2, but is at variance higher in the stack.

The two-parameter model gave a better mathematical fit (total deviation=3.47 eV) but is less physically reasonable, with $Z=0.30$ and $m_{eff}=1.4m_e$. The orbital diagram (fig. 3) is substantially the same in terms of ordering, but is compressed overall.

The HOMO–LUMO transition is rigorously forbidden in either model since both orbitals are derived from the same angular momentum state and the even parity potential function maintains their purely odd character. Molecular distortions and vibronic coupling mix even character into them and bestow a degree of allowedness on the transition, giving rise to an experimentally observed absorption onset at 1.82 eV [14]. Fig. 1 shows that the HOMO–LUMO gap is quite constant for an effective charge from about 0.3 to 1.0. The value at $Z=0.88$ is 1.40 eV, in reasonable agreement with experiment. This is in contrast to other calculations at a similar level of approximation, which typically overestimate the HOMO–LUMO gap and give results in the range of 5–7 eV [3–6,8,9].
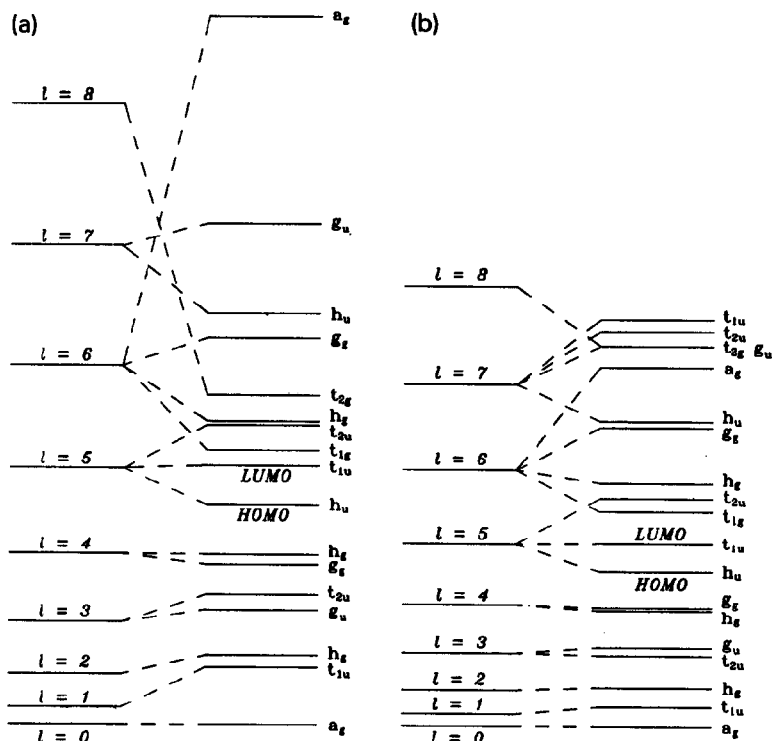
Fig. 3. Orbital diagrams for (a) one-parameter fit at $Z=0.88$ and (b) two-parameter fit at $Z=0.30$ and $m_{eff}=1.4m_e$.

4. Conclusions

Treating the π electrons of C_{60} as independent particles on a sphere perturbed by the icosahedral potential set up by the carbon atoms gives a simple description of the orbital diagram. The high symmetry of C_{60} greatly simplifies the calculation. The model is in excellent qualitative and reasonable quantitative agreement with the UV–visible spectrum and other calculations at a similar level of approximation. The parentage of each orbital is easy to discern and is the main determining factor in the allowedness of the various transitions.

Acknowledgement

References

[1] H.W. Kroto, J.R. Heath, S.C. O'Brien, R.F. Curl and R.E. Smalley, Nature 318 (1985) 162.
[2] R.C. Haddon, L.E. Brus and K. Raghavachari, Chem. Phys. Letters 125 (1986) 459.
[3] S. Larrson and A. Volosov, Chem. Phys. Letters 137 (1987) 501.
[4] F. Negri, G. Orlandi and F. Zerbetto, Chem. Phys. Letters 144 (1988) 31.
[5] P.W. Fowler, P. Lazzeretti and R. Zanasi, Chem. Phys. Letters 165 (1990) 79.
[6] G.E. Scuseria, Chem. Phys. Letters 176 (1991) 423.
[7] J.L. Martins, N. Troullier and J.H. Weaver, Chem. Phys. Letters 180 (1991) 457.

[8] M. Braga, S. Larsson, A. Rosén and A. Volosov, Astron. Astrophys. 245 (1991) 232.

[9] M. Braga, A. Rosén and S. Larsson, Z. Phys. D 19 (1991) 435.

[10] J.R. Platt, J. Chem. Phys. 17 (1949) 484.

[11] K. Ruedenberg and C.W. Scherr, J. Chem. Phys. 21 (1953) 1565.

[12] C.W. Scherr, J. Chem. Phys. 21 (1953) 1582.

[13] J.M. Hawkins, A. Meyer, T.A. Lewis, S. Loren and F.J. Hollander, Science 252 (1991) 312.

[14] S. Leach, M. Vervloet, A. Després, E. Bréheret, J.P. Hare, T.J. Dennis, H.W. Kroto, R. Taylor and D.R.M. Walton, Chem. Phys. 160 (1992) 451.

[15] H. Asie, M.M. Alvarez, S.J. Anz, R.D. Beck, F. Diederich, K. Fostiropoulos, D.R. Huffman, W. Krätschmer, Y. Rubin, K.E. Schriver, D. Sensharma and R.L. Whetten, J. Phys. Chem. 94 (1990) 8630.

[16] M. Gerloch and R.C. Slade, Ligand field parameters (Cambridge Univ. Press, 1973).

[17] E.P. Wigner, Group theory and its application to the quantum mechanics of atomic spectra (Academic Press, New York, 1959).